Spectroscopic Evidence for the Tricapped Trigonal Prism Structure of Semiconductor Clusters

Jürgen Müller,[1] Bei Liu,[2] Alexandre A. Shvartsburg,[3] Serdar Ogut,[4] James R. Chelikowsky,[4] K. W. Michael Siu,[3] Kai-Ming Ho,[2] and Gerd Gantefor[1]

[1]*Fachbereich Physik, Universität Konstanz, 78457 Konstanz, Germany*
[2]*Ames Laboratory and Department of Physics and Astronomy, Iowa State University, Ames, Iowa 50011*
[3]*Department of Chemistry and Centre for Research in Mass Spectrometry, York University, 4700 Keele Street,*
Toronto, Ontario, Canada M3J 1P3
[4]*Department of Chemical Engineering and Materials Science, University of Minnesota, Minneapolis, Minnesota 55455*
(Received 23 February 2000)

We have obtained photoelectron spectra (PES) for silicon cluster anions with up to 20 atoms. Efficient cooling of species in the source has allowed us to resolve multiple features in the PES for all sizes studied. Spectra for an extensive set of low-energy Si_n^- isomers found by a global search have been simulated using density functional theory and pseudopotentials. Except for $n = 12$, calculations for Si_n^- ground states agree with the measurements. This does not hold for other plausible geometries. Hence PES data validate the tricapped trigonal prism morphologies for medium-sized Si clusters.

Semiconductor clusters have been the focus of extensive theoretical and experimental research since the early 1980s; however, numerous controversies remain. Particular attention has been devoted to Si clusters, obviously because of the eminence of Si-based devices in the microelectronics industry (see [1]). In fact, in all cluster science the amount of work on this system is probably exceeded only by that on fullerenes. It has been found that small Si and Ge (as well as Sn) clusters are highly coordinated and compact and thus totally unrelated to the tetrahedral lattice of the bulk elements [2–5]. In spite of these efforts, the morphology and growth patterns for silicon clusters remained unknown for species larger than about a dozen atoms. Simulated annealing and chemical intuition failed to obtain conclusive structures for clusters larger than this size [6].

Recently the structures of Si clusters up to $n \sim 20$ have been characterized using the genetic algorithm [1,6–8] and its derivative—the new single parent evolution algorithm [9]. An unbiased global search employing these techniques in conjunction with density functional theory (DFT) has revealed that medium-sized ($10 \leq n \leq 20$) Si_n neutrals, cations, and anions are based mostly on the tricapped trigonal prism (TTP) Si_9 subunits [4] (Fig. 1). The same TTP building block is fundamental for Ge_n, although the exact morphologies differ [10]. Specifically, all geometries were optimized employing the local density approximation (LDA) and gradient-corrected Perdew-Wang-Becke88 (PWB) functional as implemented in the all-electron localized-basis DMOL code [11]. The double numeric basis set with polarization functions (including spin-polarization terms) has been adopted. Lowest-energy geometries located by the single-parent evolution algorithm are consistent with experiment. First, mobilities for Si_n^+ and Si_n^- in He buffer gas have been measured (including as a function of temperature) in drift tube experiments [12] with the resolution and relative accuracy of less than 1%.

The gas-phase mobility of an ion depends on its geometry. Values computed for the ground states of both Si_n^+ and Si_n^- ($n < 20$) match these data [1,8,9], which is not the case for most higher-energy isomers. Simulations reproduce all major structural rearrangements between cations and anions manifested in the size-dependent features in measured mobilities [8]. Nonetheless, different isomers are often so close in mobility that they could not be distinguished. Second, the dissociation energies/pathways calculated for Si_n^+ global minima agree with the measurements [7,9]. This shows that the search has reached true global minima in energy within the error margins of experiment and calculation but does not prove the actual geometries. Third, the ionization potentials calculated for ground state Si_n track the experimental trend [1]. The above comparisons involving different observables support the theoretical findings strongly. However, the
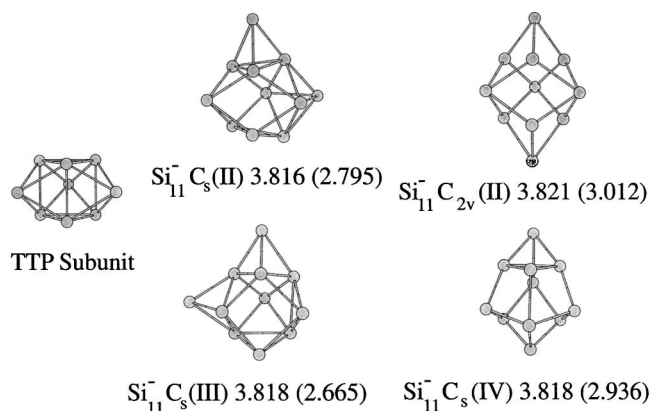

FIG. 1. Four near-degenerate lowest energy Si_{11}^- isomers that have vertical detachment energies close to the measured value. We list calculated cohesive energies (PWB in eV/atom) and VDEs (LDA, eV) in parentheses. The TTP structural unit common for the medium-sized semiconductor clusters is depicted in front.

most direct evidence for proposed geometries would be provided by some form of spectroscopy.

Photoelectron spectroscopy is a powerful tool for the structural characterization of free atomic clusters [13–16]. It reflects the electronic structure of neutrals at the anion geometry. Experimentally, the anion is photoexcited above the detachment threshold and the energy of released electrons is measured. One can pinpoint the threshold and the maximum of detachment efficiency. Assuming zero initial temperature, the first quantity ideally indicates the adiabatic electron affinity (AEA) and the second is the vertical detachment energy (VDE)—the energy needed to remove an electron from the HOMO without relaxing the rest of the system. In practice, the threshold sets the upper limit for AEA, so VDEs are generally more accurate than AEAs (the VDEs reported below are defined by the position of first maximum in detachment efficiency). Depending on the photon energy, some electronic orbitals below the HOMO may also be revealed. In the best-case scenario, a vibrationally resolved spectrum exhibits certain normal modes of the cluster. Unlike mobility measurements, photoelectron spectroscopy probes both the geometry and the electronic structure. In metal clusters, the HOMO-LUMO gap (band gap) normally decreases with increasing size as a consequence of electronic level quantization in a cavity. It has been thought that the highly coordinated bonding in Si clusters renders them "metallic." A direct examination of electronic structure would determine if this is true.

Photoelectron spectra (PES) have been obtained for Si_n^- up to $n = 12$ [13–16], but vibrational resolution could be achieved only for $n \leq 7$ [14,15]. Comparison of the measured frequencies with those computed for trial geometries has identified Si_3^- as a triangle, Si_4^- as a rhombus, and Si_5^- and Si_7^- as trigonal and pentagonal bipyramids, respectively. Matrix-isolated neutrals have the same morphologies [17]. Absent vibrational resolution, cluster structures could still be assigned by matching the observed electronic band profiles with those simulated for plausible candidate isomers [18,19]. Using this approach, the geometries of Si_6^- and Si_{10}^- have been determined as the C_{2v} (II) bicapped tetrahedron and the C_{3v} tetracapped trigonal prism. As predicted in theory, the structure of Si_6^- differs from that of the neutral D_{4h} tetragonal bipyramid [18]. Summarizing, Si_n^- structures for $n < 7$ and $n = 10$ have already been characterized by PES. These geometries are global minima in calculations [4,18,19] and agree with mobility measurements [1,8]. Except for Si_{10}^-, these structures contain no TTP units. Hence, there has been essentially no spectroscopic evidence for the TTP-based growth of semiconductor clusters.

Here we report and assign the photoelectron spectra measured for Si_n anions with $n \leq 20$. The apparatus used in these experiments has already been described [20]. Briefly, clusters were generated in a pulsed arc source and cooled in a 30-cm long extender with a diameter of 4–8 mm. This cooling was critical for the observation of structured spectra. Cold anions were mass separated in a time-of-flight mass spectrometer and crossed a laser beam. The detached electrons were collected using a "magnetic bottle" electron spectrometer. High photon energy of 6.4 eV allowed us to image a number of electronic levels below the HOMO, which provided rich information for structural assignments. Spectra measured for $n \geq 8$ are presented in Fig. 2. In the size region of overlap ($n \leq 12$), our results closely reproduce the published data [13,16].

To sort through a large number of trial structures efficiently, we first compared only the calculated VDEs with the experiment. These have been calculated in both LDA and PWB (using DMOL) by subtracting the energy of an anion from that of the neutral at the same geometry. For species exhibiting a reasonable agreement, the complete PES were simulated employing a real space LDA pseudopotential calculation [18,19]. In these codes, the cluster temperature (T) is adjusted to fit the width of measured features. This is not the actual temperature of clusters, because factors besides thermal broadening contribute to the total peak width. Thus it is not surprising that the measurements are fit best assuming $T \sim 1000$ K, a value way above the vibrational cluster temperature of ~ 300 K.

VDEs calculated for the Si_n^- global minima and a number of other important structures are compared with the measured values in Fig. 3. The VDEs for ground states (but almost no other isomers) are in excellent agreement
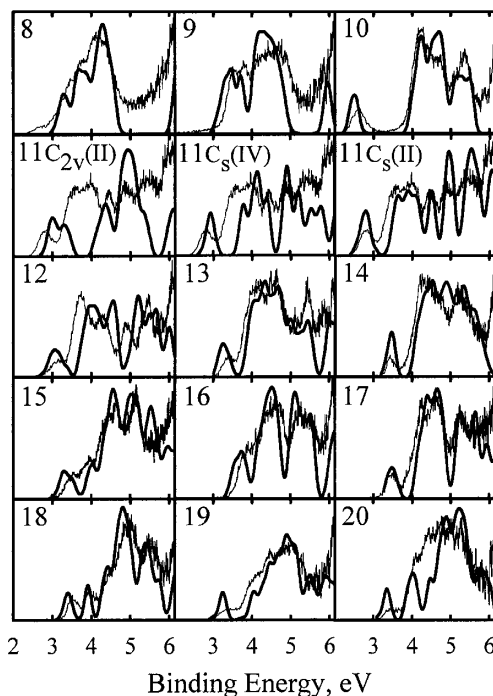

FIG. 2. Photoelectron spectra for Si_n anions ($n = 8-20$), measurements (thin lines), and LDA simulations (thick lines). Calculations have been performed for Si_n^- ground states (depicted in Refs. [8,9] and in Fig. 1) assuming a cluster "temperature" of 1000 K. For $n = 11$, we also show the PES simulated for low-energy C_s (II) and C_s (IV) isomers.
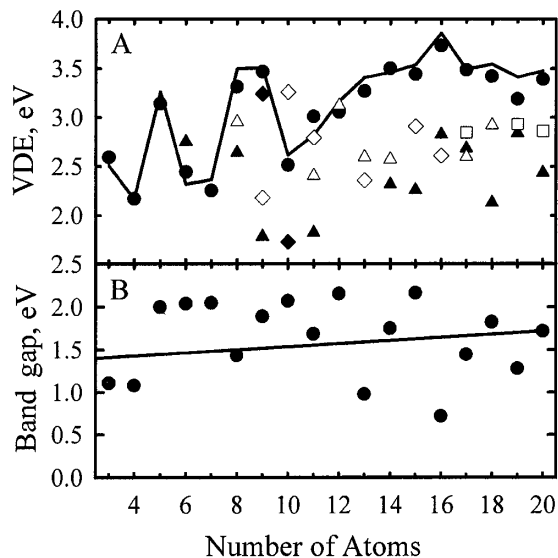
FIG. 3. (A) Vertical detachment energies of Si_n anions ($n \leq 20$). The line indicates our measurements. The symbols mark values calculated using LDA for a variety of geometries: the lowest-energy Si_n^- [8,9] (circles, C_{2v} structure adopted for Si_{15}^-); isomers that are global minima for Si_n [6,8,9] when different from Si_n^- [filled triangles, $Si_{11}C_{2v}$ (I) assumed]; isomers that are global minima for Si_n^+ [1,8,9] when different from both Si_n^- and Si_n (empty triangles, C_s geometry assumed for Si_8^+); some other low-energy TTP-based species: $Si_9^-C_{2v}$ (II) distorted TTP [8,22], $Si_{10}^-C_{4v}$ bicapped tetragonal antiprism [19], $Si_{11}^-C_s$ (II) [8,25], $Si_{13}^-C_{3v}$ capped trigonal antiprism [8,26], $Si_{15}^-C_s$ (III) and $Si_{16}^-C_{2h}$ (I) [8] (empty diamonds); octahedron-based structures [4,8] $Si_9^-C_s$ (I) and $Si_{10}^-T_d$ (filled diamonds); and near-spherical [8] $Si_{17}^-C_2$, $Si_{19}^-C_{2v}$, and $Si_{20}^-C_s$ (squares). VDEs computed using PWB are within 0.1–0.2 eV of LDA values, typically (but not always) on the lower side. (B) Band gaps calculated (by PWB) for the lowest-energy Si_n neutrals. The line is the first-order regression through the data.

with experiment. Our analysis of PES for $n \leq 7$ and $n = 10$ agrees with the literature [18,19]. For Si_{10}^-, both the C_{4v} bicapped tetragonal antiprism and T_d tetracapped octahedron (respectively, the second and third lowest-energy isomers) could be ruled out as their VDEs are off by ~1 eV. (We estimate the combined error margin of experiment and calculations to be within 0.3 eV.) The case of $n = 8$ is particularly interesting, as the ground states for Si_8^+, Si_8, and Si_8^- are entirely dissimilar: C_1/C_s capped pentagonal bipyramid [1], C_{2h} distorted bicapped octahedron [1,2], and C_{2v} (or C_{3v}) tetracapped tetrahedron [4], respectively. The mobilities calculated for all three species match the measurement for Si_8^- within 1%, so the structures could not be distinguished [8]. It is, however, clear from Fig. 3 that the geometry observed is C_{2v}/C_{3v}, as predicted by theory [4]. Four low-energy geometries for $n = 9$ have been extensively discussed: the C_{2v} (I)/C_1 capped Bernal's structure [21], C_{2v} (II) distorted TTP [22], C_s (I) tricapped octahedron [2,4], and another distorted TTP, C_s (II) [4]. The ground state for Si_9^- is C_s (II) [4,8],

but that for Si_9 and Si_9^+ is C_{2v} (I) [1]. This rearrangement has been supported by mobility measurements, which exclude the C_s (II) isomer for Si_9^+, C_{2v} (I) and C_{2v} (II) for Si_9^-, and C_s (I) for both charge states [1,8]. PES confirms the C_s (II) morphology, as the VDEs for C_{2v} (I), C_{2v} (II), and C_s (I) isomers all fail to match the measurement. Si_9 TTP anions have recently been observed in bulk as a part of the crystal structure of $Rb_{12}Si_{17}$ [23]. DFT global minima for $n = 11$ are the C_s (I) structure for the cation [1], C_s (I) or C_{2v} (I) for the neutral [1,24], and C_{2v} (II) for the anion [8] (Fig. 1). Mobilities calculated for all three geometries are within 1% of the experiment for either Si_{11}^+ or Si_{11}^- [1,8], so no structural assignment can be made. We could elucidate the neutral as C_{2v} (I) on the basis of ionization potential [1]. VDE measured for Si_{11}^- matches that for the C_{2v} (II) isomer, but not those for either C_s (I) or C_{2v} (I). C_s (II) geometry [25] and hitherto unknown C_s (III) and C_s (IV) structures (Fig. 1) that are all virtually degenerate [8] with Si_{11}^- C_{2v} (II) could not be ruled out, as their VDEs are also close to the measurement and they have right mobilities. The VDE of C_{2v}, the ground state for Si_{12} and Si_{12}^- [8], fits the experimental data. However, so does the VDE of the C_s geometry, the global minimum for Si_{12}^+ [1]. As the mobilities calculated for C_s and C_{2v} morphologies are virtually equal, the structural distinction between Si_{12}^+ and Si_{12}^- remains unverified [8]. The VDE for the C_s structure, the ground state for Si_{13} and Si_{13}^- [8], agrees with the measurement. The detachment energies for other isomers that we considered are significantly lower, including that for the C_{3v} capped trigonal antiprism claimed at some point [26] as the global minimum for Si_{13}. The VDE of C_s (II), the ground state for Si_{14}^- [8], matches the measurement, whereas that of the C_s (I) isomer, the lowest-energy neutral [1], does not. Neither the C_s (III) structure found to be the global minimum for Si_{15}^- in [8], nor the C_{3v} isomer, the ground state for Si_{15} and Si_{15}^+ [1], fits the experiment. In DFT, the C_s (III) [8] and new $Si_{15}^-C_{2v}$ [9] morphologies are essentially degenerate (the C_{2v} is lower in energy by 0.11 eV in LDA but higher by 0.03 eV in PWB). However, PES clearly shows that only the C_{2v} isomer is produced. The VDE of the lowest-energy Si_{16} anion (C_s) agrees with the measurement, but that of C_{2h} (II), the ground state for Si_{16} and Si_{16}^+ [1], does not. The situation for $n = 17$ and 18 is similar.

Clearly the detachment energies are quite sensitive to cluster geometries. VDEs for all Si_n^- global minima ($n \leq 20$) agree with the experiment. This is the case for only four out of many higher-energy isomers that we found in this size range, and these exceptions are limited to $n = 11$ and 12. This selectivity is understandable considering that the second lowest Si_n^- isomers in the $n = 13$–19 range (except $n = 15$) lie above the best by 0.2 eV at least. PES simulated for global minima are superimposed on measured spectra in Fig. 2. Except for

$n = 11$, 12, and (to some extent) 20, simulations clearly reproduce all significant features distinguishable in the PES. The mobility computed for the lowest-energy Si_{20}^- located does not match the measurement [8]. Thus perhaps the ground state for this system is yet to be found. PES have been simulated for Si_{11}^- and Si_{12}^- geometries that lie within a few meV/atom above the calculated global minima and have correct VDEs. Spectra calculated for $Si_{11}^- C_s$ (III), $Si_{11}^- C_s$ (IV), and $Si_{12}^- C_s$ do not fit the measurements. However, the PES for $Si_{11}^- C_s$ (II) agrees with the experiment perfectly (Fig. 2). Except for $n = 10$ and 11, the observed Si_n^- isomers are those with the highest VDEs. This is because the lowest-energy cluster geometries tend to have the lowest-lying HOMOs and thus the highest VDEs.

PES for $n = 8$ and 9 differ from those for other $n \leq 20$ in that they often exhibit ledges at energies down to ~ 2.5 eV. The origin of these features has not been explained, but they are not always reproducible [13,16]. This caused a large spread of values reported for the electron affinities of Si_8 and Si_9 [16], depending on whether the ledges are viewed as a part of the PES or ignored. Such ledges normally indicate a geometry with low VDE that is a minor component of the isomeric mixture, but no low-energy Si_8^- and Si_9^- isomers with the requisite VDEs have been found. Cluster anions are produced in a laser vaporization source by attachment of electrons to neutrals. A cluster may then assume the lowest-energy anion geometry or retain the neutral structure, depending on the isomerization barrier and source conditions. VDEs calculated for Si_8^- and Si_9^- isomers relaxed from the ground state neutrals [6] are, respectively, 2.45 eV and 2.67 eV (PWB); hence, the observed ledges are plausibly due to these structures. Si_n^- and Si_n global minima also differ for many n other than 8 and 9. However, in those cases the structural difference between the Si_n and Si_n^- ground states is less drastic, and the barriers to rearrangement should be lower.

The ability of our calculations to reproduce experimental PES gives us the confidence to compute the HOMO-LUMO gaps for Si_n neutrals ($n \leq 20$). These clearly do not decrease with increasing n as would be the case for metallic species (Fig. 3).

In conclusion, we measured the photoelectron spectra of Si_n anions with $n \leq 20$. Results for a number of low-energy isomers found by a global search were modeled using DFT. For all $n \leq 19$, except $n = 12$, PES simulated for the Si_n^- global minima are in excellent agreement with the experiment. This agreement is highly specific to particular morphologies. For example, the ground states for Si_n with $n = 6$, 8, 9, 11, and 14–20 as well as Si_n^+ with $n = 8$, 9, and 11–20 differ from those for Si_n^-. Although all these geometries are also built on the tricapped trigo-

nal prism motif, none of them fits the measured PES. The band gap does not decrease with increasing cluster size as one would expect for metallic clusters.

[1] B. Liu *et al.,* J. Chem. Phys. **109**, 9401 (1998).
[2] K. Raghavachari and C. M. Rohlfing, J. Chem. Phys. **89**, 2219 (1988).
[3] P. Ballone *et al.,* Phys. Rev. Lett. **60**, 271 (1988).
[4] K. Raghavachari and C. M. Rohlfing, J. Chem. Phys. **94**, 3670 (1991).
[5] A. A. Shvartsburg and M. F. Jarrold, Phys. Rev. A **60**, 1235 (1999).
[6] K. M. Ho *et al.,* Nature (London) **392**, 582 (1998).
[7] A. A. Shvartsburg *et al.,* Phys. Rev. Lett. **81**, 4616 (1998).
[8] A. A. Shvartsburg *et al.,* J. Chem. Phys. **112**, 4517 (2000).
[9] I. Rata *et al.,* Phys. Rev. Lett. **85**, 546 (2000).
[10] A. A. Shvartsburg *et al.,* Phys. Rev. Lett. **83**, 2167 (1999).
[11] DMOL package, V96.0/4.0.0, MSI, San Diego, 1996.
[12] R. R. Hudgins *et al.,* J. Chem. Phys. **111**, 7865 (1999).
[13] O. Cheshnovsky *et al.,* Chem. Phys. Lett. **138**, 119 (1987).
[14] C. C. Arnold and D. M. Neumark, J. Chem. Phys. **99**, 3353 (1993); **100**, 1797 (1994); C. Xu *et al.,* J. Chem. Phys. **108**, 1395 (1998).
[15] G. Schulze Icking-Konert *et al.,* Surf. Rev. Lett. **3**, 483 (1996).
[16] H. Kawamata *et al.,* J. Chem. Phys. **105**, 5369 (1996); R. Kishi *et al., ibid.* **107**, 10 029 (1997).
[17] E. C. Honea *et al.,* Nature (London) **366**, 42 (1993).
[18] N. Binggeli and J. R. Chelikowsky, Phys. Rev. Lett. **75**, 493 (1995).
[19] J. R. Chelikowsky and N. Binggeli, Mater. Sci. Forum **232**, 87 (1996); S. Ogut and J. R. Chelikowsky, Phys. Rev. B **55**, R4914 (1997).
[20] C. Y. Cha, G. Gantefor, and W. Eberhardt, Rev. Sci. Instrum. **63**, 5661 (1992).
[21] I. Vasiliev, S. Öğüt, and J. R. Chelikowsky, Phys. Rev. Lett. **78**, 4805 (1997).
[22] J. C. Grossman and L. Mitas, Phys. Rev. Lett. **74**, 1323 (1995).
[23] V. Queneau, E. Todorov, and S. C. Sevov, J. Am. Chem. Soc. **120**, 3263 (1998).
[24] K. Raghavachari and C. M. Rohlfing, Chem. Phys. Lett. **167**, 559 (1990).
[25] A. Sieck *et al.,* Phys. Rev. A **56**, 4890 (1997).
[26] U. Rothlisberger, W. Andreoni, and P. Giannozzi, J. Chem. Phys. **96**, 1248 (1992).